

# We are IntechOpen, the world's leading publisher of Open Access books Built by scientists, for scientists

4,800

Open access books available

122,000

International authors and editors

135M

Downloads

Our authors are among the

154

Countries delivered to

TOP 1%

most cited scientists

12.2%

Contributors from top 500 universities



WEB OF SCIENCE™

Selection of our books indexed in the Book Citation Index  
in Web of Science™ Core Collection (BKCI)

Interested in publishing with us?  
Contact [book.department@intechopen.com](mailto:book.department@intechopen.com)

Numbers displayed above are based on latest data collected.  
For more information visit [www.intechopen.com](http://www.intechopen.com)



---

# Lumped-Element Modeling for Rapid Design and Simulation of Digital Centrifugal Microfluidic Systems

---

Mahdi Mohammadi, David J Kinahan and  
Jens Ducreé

Additional information is available at the end of the chapter

<http://dx.doi.org/10.5772/62836>

---

## Abstract

Since the 1990s, centrifugal microfluidic platforms have evolved into a mature technology for the automation of bioanalytical assays in decentralized settings. These “Lab-on-a-Disc” (LoaD) systems have already implemented a range of laboratory unit operations (LUOs) such as sample loading, liquid transport, metering, aliquoting, routing, mixing, and washing. By assembling these LUOs in highly functional microfluidic networks, including sample preparation and detection, a sizable portfolio of common test formats such as general chemistry, immunoassays/protein analysis, nucleic acid testing, and cell counting has been established. The availability of these bioanalytical assay types enables a broad range of applications in fields such as life-science research, biomedical point-of-care testing and veterinary diagnostics, as well as agrifood, environmental, infrastructural, and industrial monitoring.

Recently, a new method of the so-called “event-triggered” flow control has been developed which is independent of the spin rate. These valves, which function in a handshake mode as opposed to the typically batchwise liquid transfers on the “Lab-on-a-Disc” (LoaD) platform, assume a similarly pivotal role as relays and transistors in digital electronics, allowing conditional, logical (flow) control elements. This chapter will describe the modeling of this new generation of “digital” centrifugal microfluidic systems with low-dimensional, lumped-element simulations which have already been instrumental to the modern success story of modern microelectronics.

**Keywords:** lumped-element simulation, centrifugal microfluidics, lab-on-a-disc, event-triggered flow control, valving

---

## 1. Introduction

The centrifugal microfluidic platform has evolved into mature technology platform which has already proven to open significant market opportunity [1–5]. A large number of groups working on such LoD systems in industry has already convincingly demonstrated the capability to integrate, automate, parallelize, and miniaturize a wide range of common bioanalytical test formats for detecting targets such as small molecules, proteins/antibodies, nucleic acids, and cells. Applications span from decentralized biomedical point-of-care diagnostics, veterinary medicine and agrifood, to the surveillance of the environment and infrastructures.

Based on the recently introduced, event-triggered flow control scheme [6, 7], highly functional microfluidic circuits can be assembled in a modular fashion from a limited set of LUOs to implement a broad repertoire of multi-step, multi-reagent bioassay protocols in a sample-to-answer fashion. Furthermore, it has been demonstrated that the chips could be progressively miniaturized to significantly enhance integration density (i.e., the number of assay steps and/or tests per disc) and thus boost the overall cost efficiency and functionality of the LoD platform.

Similar to integrated circuits in microelectronics, a microfluidic network can be modeled by lumped-element descriptors. Instead of a finely meshed 3-dimensional lattice, the Lab-on-a-Disc systems are described by a low number of parameters such as pressure head (voltage source), flow resistance (electric resistance), and compressibility (capacitance). This reduced-dimension method can be utilized for fast design and simulation of microfluidic systems that are composed of a library of functional units.

After the introduction (Section 1), the hydrodynamic principles of centrifugal microfluidics are presented (Section 2) before outlining digital flow control schemes (Section 3). Next, the concept of lumped-element simulation in event-triggered centrifugal microfluidic networks is developed (Section 4).

## 2. Centrifugal hydrodynamics

The rotationally controlled microfluidic “Lab-on-a-Disc” platform is based on (the volume density of) the centrifugal force

$$f_{\omega} = \rho r \omega^2 \quad (1)$$

the Euler force

$$f_E = \rho r . d\omega / dt \quad (2)$$

and the Coriolis force [1]

$$f_c = 2\rho\omega v \quad (3)$$

where  $\rho$  is a fluid density on a rotating platform,  $\omega = 2\pi v$  the angular velocity with the frequency of rotation  $v$ ,  $r$  is a distance from a central axis, and  $v$  represents the speed of flow. All forces act in the plane of the disc and scale with the angular velocity  $\omega$  directly impacts these three forces.

The centrifugal force (Eq. (1)) translates into an equivalent centrifugal pressure

$$\Delta p_\omega = \rho\Delta r\bar{r}\omega^2 \quad (4)$$

and an average flow velocity

$$V = \frac{D_h^2 \rho \Delta r \omega^2 \bar{r}}{32\mu L} \quad (5)$$

of the liquid in the channel [5] featuring the hydraulic diameter  $D_h = 4A/P$  with the  $A$ ,  $P$ , and  $L$ , its cross-sectional area  $A$ , wetted perimeter of the channel  $P$ , and length  $L$ . The fluid viscosity is denoted by  $\mu$ , the mean radial position by  $\bar{r} = (r_2 + r_1)/2$ , and the radial length by  $\Delta r = (r_2 - r_1)$ .

Air pockets, which often arise accidentally or strategically during priming, can be compressed by the hydrostatic pressure head of a liquid column (4) in a more central position. This centrifugally induced pressure compresses the enclosed gas volume

$$P_c = P_0 \frac{1}{1 - \Delta V / V} \quad (6)$$

according to Boyle's law [6] where  $P_c$  represents the pressure of the gas in the pneumatic chamber,  $V$  is the total volume of the pneumatic chamber, and  $\Delta V$  denotes a reduction of gas volume due to filling of liquid in the pneumatic chamber.

### 3. Digital flow control schemes

Flow control is instrumental for orchestrating sequential liquid handling on the LoAD platforms where all volumes are subjected to the same centrifugal field (Eq. (1)). Such flow control can be categorized into rotationally actuated and instrument-supported schemes.

Instrument-supported valves involve some stationary modules (other than the platform innate spindle motor). To switch a valve, these "lab-frame" elements interact with the disc cartridge,

either at rest or during spinning. The actuation can be powered by pneumatic pressure sources [8–9], heating of phase-change materials [10–13], or even varying the chip orientation with respect to the radial direction [14–16]. While these may provide enhanced and more flexible control, these active valving mechanisms typically involve additional instrumentation, maintenance, cost, and susceptibility to failure.

Rotationally actuated valves are far more common and are considered more suitable for deployment of inexpensive point-of-use applications. Through varying the rotationally induced fields relative to the statically defined forces such as interfacial or membrane tension, the force equilibrium at a fluid element can be unbalanced. Such static forces can be implemented by capillary action [17–21], dissolvable films (DFs) [22–23], burstable foils [24], elastomeric membranes [25], dead-end pneumatic chambers [26], siphons [27–29], and pneumatically enhanced centrifugo-pneumatic siphons (CPSVs) [30–33].

In particular the popular, rotationally actuated capillary “burst” valves are strongly dependent on physicochemical properties such as geometry, surface roughness, and contact angle; hence, valve performance is intimately linked to manufacturing fidelity. The often rather poor reproducibility and stability of these effects translate into a significant “smearing” of the burst frequencies. For serial flow control which is common in bioanalytical protocols, rather wide, non-overlapping bands of the spin rate have to be reserved for each assay step. As the maximum spin rate is practically limited by the motor power and safety, this imposes a practical limit on the number of sequential LUOs which can be rotationally controlled by a spindle motor.

Event-triggered valving circumvents this restriction [6–7]. Here, the arrival of liquid at defined locations on the disc coordinates a sequential opening of valves; valve actuation is thus decoupled from changes in the spin rate and support instrumentation. So far, event-triggered valving has been based on dissolvable film (DF) membranes [22], [23], [34], [35] and, in function, can be described akin to an electrical relay. The architecture of the disc determines the order of valve actuation, while the timing is controlled by the dissolution of these membranes. It has been shown that event-triggered schemes can also implement logical flow control elements such as AND and OR conditions [6], thus enabling a modular system design similar to electronics. Developing the lumped-element tool for the simulation, digital centrifugal microfluidic systems can generate a broad scope of applications, thus mitigating development risks, upfront investment, and time to market.

The basic event-triggered valve is composed of a pneumatic chamber sealed by the restrained liquid and two dissolvable films called the load film (LF) and the control film (CF). The geometry of the pneumatic chamber is designed so that, at the spin rates typical for the centrifugal platform, the restrained liquid cannot be pumped into contact with the LF or CF by compressing the trapped air within the pneumatic chamber. Similarly, the section of the chamber connecting the LF and CF extends radially inward of the restrained liquid. When the CF is wetted and dissolved by an ancillary liquid, the pneumatic chamber is vented so the main liquid contacts and thus opens the LF.

However, the connecting channel between the LF and CF acts as a geometric barrier which prevents the liquid escaping through the disrupted CF. Thus, in this configuration, the CF acts analogous to the control line of an electrical relay and the LF to the load line. This basic configuration can then be arranged into a complex fluid network where valves sequentially cascaded; the flow released from the first valve triggers the subsequent “ancillary liquid.” Importantly, the interval between valve actuations is governed by the aggregate time of membrane dissolution and liquid transfer.

Alongside the basic configuration (**Figure 1**), the conditions of valve actuation can be altered by changing the arrangement of the CF. For example, locating the CF such that it can only be wetted when two or more upstream “ancillary liquid” volumes have been released (Figure 1) establishes a Boolean AND condition. Similarly, by designing a valve with two CFs where wetting one or the other will trigger the valve, we create a Boolean OR condition (**Figure 2**). Finally, locating two CFs in close proximity so they can be reached by a single ancillary liquid can simultaneously open two pneumatically connected valves and thus can represent parallel valve actuation (**Figure 3**).

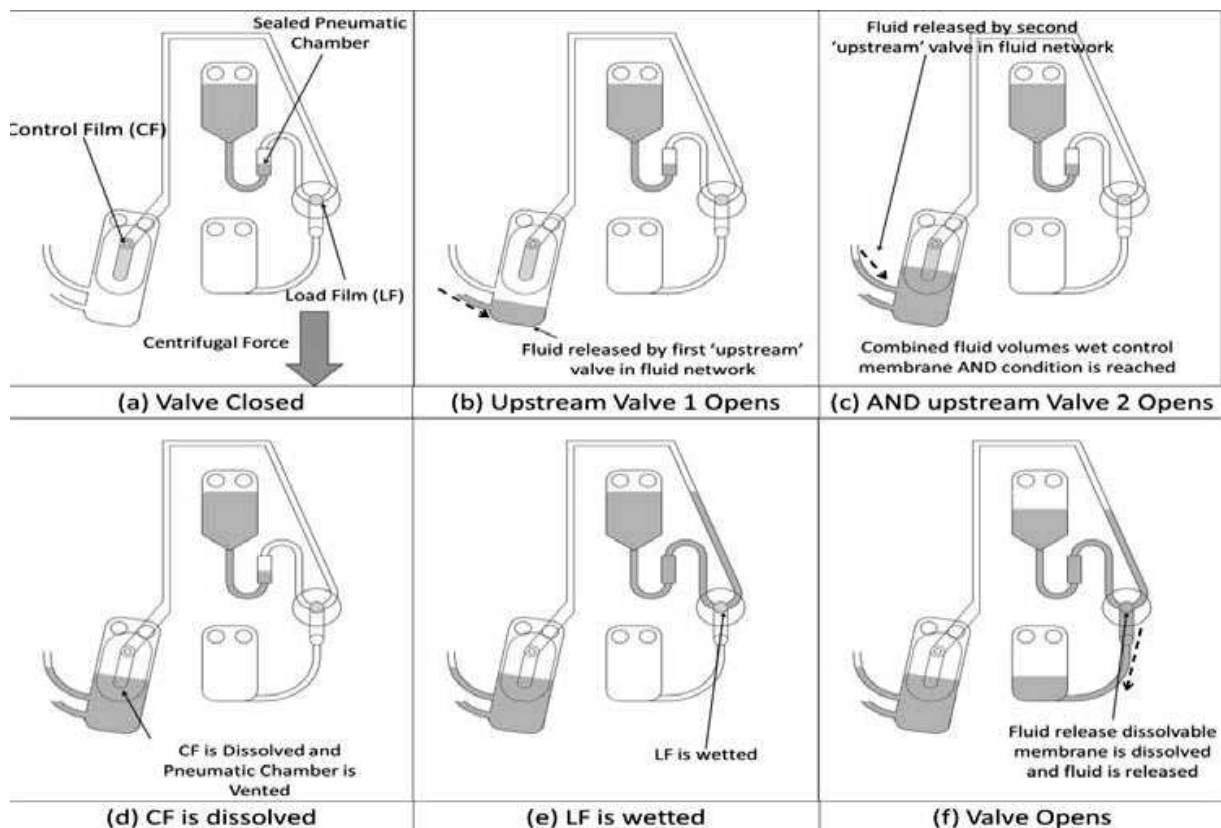


**Figure 1.** Schematic demonstrating the basic event-triggered configuration and also showing the Boolean AND release mechanism (a) Valve closed, (b) upstream valve 1 opens (c) AND upstream valve 2 opens, (d) CF is dissolved, (e) LF is wetted, (f) Valve opens.

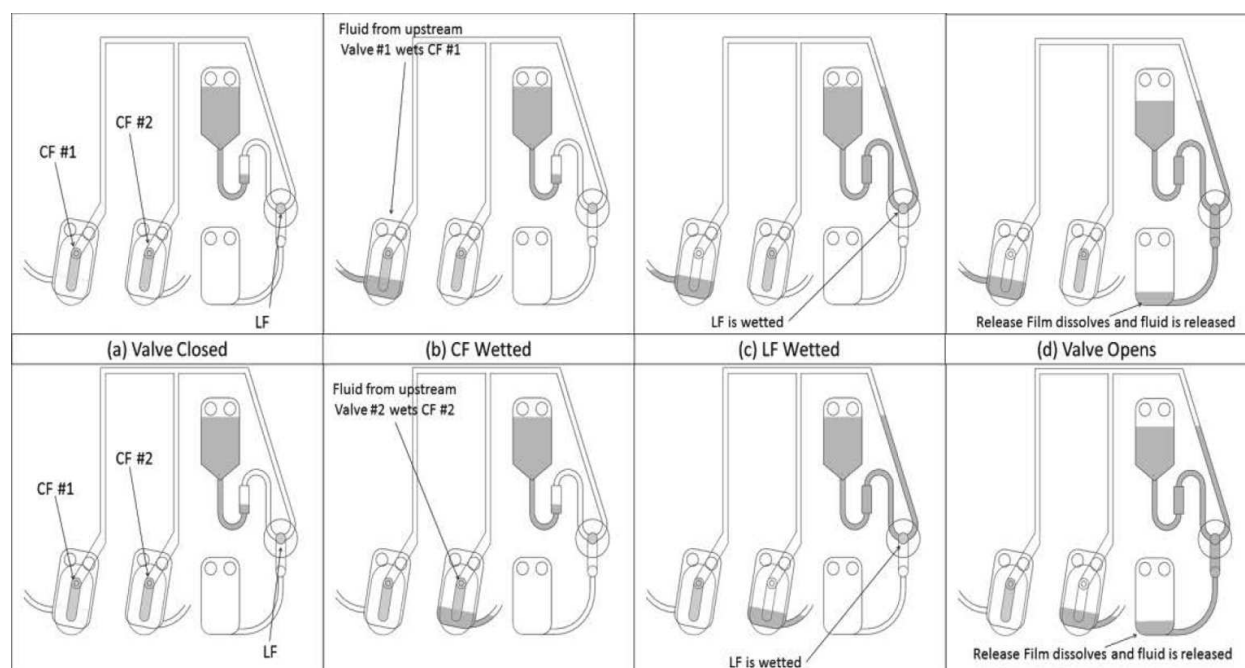


**Figure 2.** Schematic illustrating the OR conditional release mechanism. The top pane shows the valve actuation triggered by liquid movement to one chamber and the lower pane shows the valve actuation triggered. (a) Valve closed, (b) CF wetted, (c) LF wetted, (d) Valve opens.

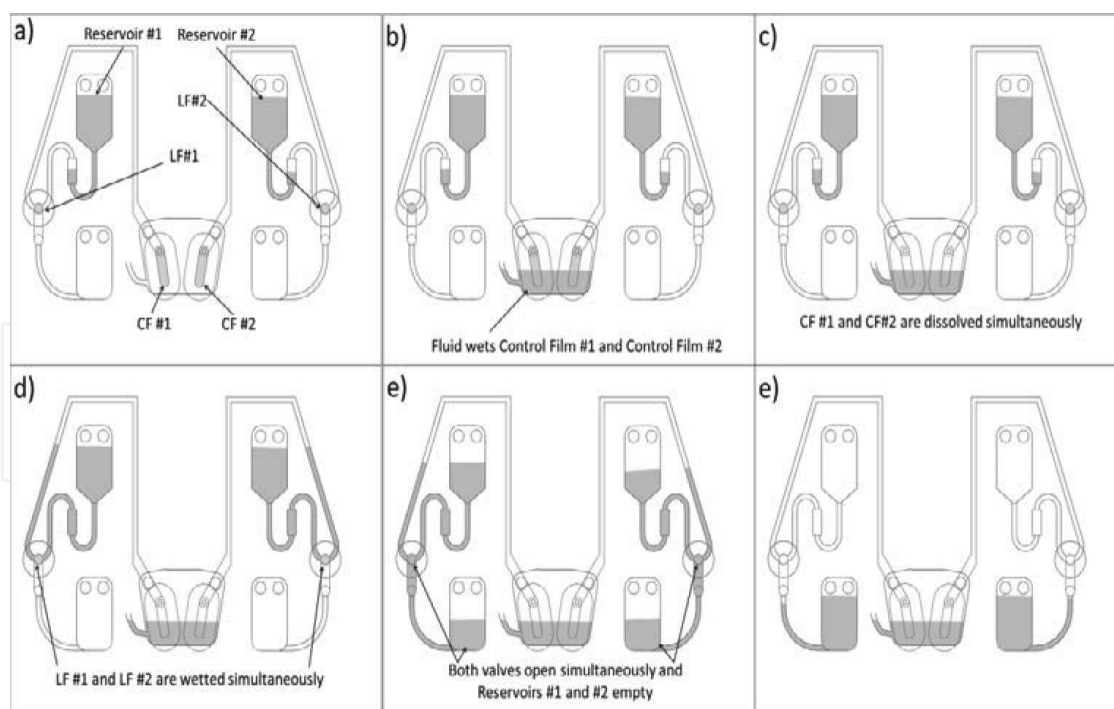


**Figure 3.** Schematic illustrating the OR conditional release mechanism. The top pane shows the valve actuation triggered by liquid movement to one chamber and the lower pane shows the valve actuation triggered. (a) Valve closed, (b) CF wetted, (c) LF wetted, (d) Valve opens, (e) Both valves open simultaneously and Reservoirs #1 and #2 empty, (f) Reservoirs #1 and #2 empty.

#### 4. The concept of lumped-element simulation in digital, event-triggered centrifugal microfluidic networks

The rapid evolution of microelectronics (following Moore’s law) has been leveraged by the trinity of miniaturization, fabrication, and, last but not least, large-scale system integration (LSI). The breathtaking progress within these tightly intertwined factors has tremendously reduced production costs and seminally enhanced system performance. This is clearly visible when looking back over the last decades when microelectronic devices took the road from very clumsy, maintenance-intensive, multi-million dollar machines sparsely scattered around the globe to the sleek, ubiquitous, and quite affordable digital gadgets people even carry in their pockets. The unprecedented commercial success story of microelectronics has been enabled by seminal advances in microfabrication as well as the capability to generate complex functional architectures from a limited set of base modules such as capacitors and transistors. These simple modules are composed into sophisticated functional networks by lumped-element model software. We have developed a new type of “digital” LoAD platform which follows a similar design paradigm to implement different types of bioanalytical tests, e.g., for small molecules, proteins, antibodies, DNA, and cells [6].

Over the past decades, simulation has a key role in developing new products. The common simulation methods are FEA (finite element analysis), CFD (computational fluid dynamic), and MBS (multi-body systems). In principle, these mesh-based simulation methods are very accurate. Nevertheless, these numerical tools display serious limitations, for instance, that they tend to be very time-consuming; in particular for more complex networks, also the grid size and proper boundary conditions impact the result (mesh dependency). Therefore, simplified geometries are required for keeping computation times and common convergence issues at bay; lumped-element simulation was proposed to simplify analysis based on electric circuit elements; this method is quite fast and fit for swift parameter optimization; in addition, these methods could simulate serial and parallel multi-element architectures [36].

The centrifugal flow control elements and their combination of complex microfluidic circuitry translate into equivalent, lumped-element descriptors. Each lumped element exhibits certain free parameters, for instance, corresponding to resistances or capacitances. In microfluidics, these parameters typically relate to geometries, e.g., the channel cross section, as well as hydrodynamic and mechanical properties such as the viscosity and compressibility of the fluids and the flexibility of the ducts. Lumped-element analogies for the different environments are listed in **Table 1**.

	Effort (e)	Flow (f)	Inertance	Capacitance	Resistance	Displacement (q)	Node law	Mesh law
Electricity,..	Voltage (V)	Current (I)	Inductor (L)	Capacitor (C)	Resistor (R)	Charge (Q)	KCL	KVL
Fluidic	Pressure (P)	Flow (q)	Inertance (M)	Fluid capacitance	Flow resistance	Volume (V)	Mass conservation	Pressure is relative



	Effort (e)	Flow (f)	Inertance	Capacitance	Resistance	Displacement	Node law	Mesh law
				(C)	(R)	(q)		
Mechanics	Force (F)	Velocity (V)	Mass (m)	Spring (K)	Damper (b)	Displacement (x)	Continuity of space	Newton's 2nd law
Thermal	Temp. diff ( $\Delta T$ )	Heat flow	-	Heat capacity (mcp)	Thermal resistance (R)	Heat (Q)	Heat energy conservation	Temperature is relative

**Table 1.** Physical lumped-element analogies in different environments.

For a given microfluidic network and spin rate protocol, the lumped-element simulation of microfluidic systems allows to calculate pressure distribution, flow rate, and timing. Parallel simulation and parameter sweep for efficient design generation of microfluidic systems represent further advantages of lumped-element simulation. In addition, its computational simplicity and fast convergence mean it can also be applied to “real-time” active control of microfluidic processes. Utilizing this real-time graphical simulation to monitor filling level and aliquoting timing along the LUOs in multi-step, multi-reagent bioassay protocols will constitute an important milestone because it would allow the evaluation of the functional operation of the LoaD device without any further fabrication and experimental processes.

This lumped-element simulation in different environments is illustrated by the equivalent electric circuit elements comprising a resistor, a capacitor, and a diode, and the required relations for lumped-element simulation are presented in the following:

#### 4.1. Kirchhoff's current law (KCL) [37]

The material balance equation, flow-in equal flow-out at any given node in the microfluidic network.

$$\sum_i I_i = 0 \xrightarrow{\text{At each nodes}} \sum_i q_i = 0 \rightarrow q_{in(1)} + q_{in(2)} + \dots = q_{out(1)} + q_{out(2)} + \dots \quad (7)$$

#### 4.2. Kirchhoff's voltage law (KVL) [31]

The sum of pressure differences around a microfluidic loop must be zero.

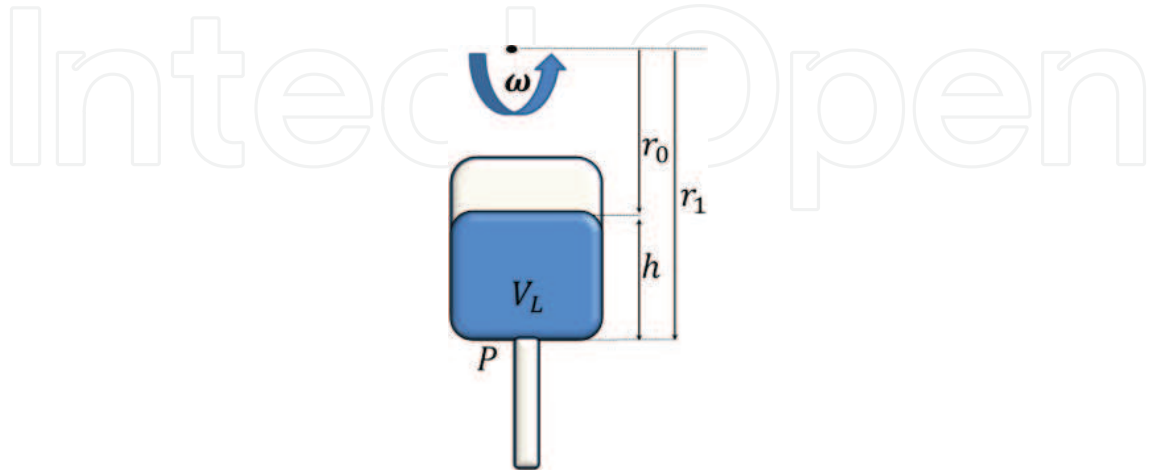
$$\sum_i V_i = 0 \xrightarrow{\text{In closed loop}} \sum_i P_i = 0 \quad (8)$$

#### 4.3. Capacitance

Increasing charge storage results in increasing voltage in an electrical capacitor and increasing fluid leads to increase pressure in the reservoir (fluid capacitor).

$$V_L = C.P \quad (9)$$

The force at the bottom of storage due to the weight is  $mg = \rho V_L g$  which constant earth gravitational replaces by artificial gravity field  $g = \bar{r}\omega^2$  in the centrifugal microfluidic system.



$$P = \frac{\rho V_L g}{A} = \rho g h \rightarrow P = \frac{\rho V_L \bar{r} \omega^2}{A} = \rho \bar{r} \omega^2 (r_1 - r_0)$$

$$V_L = \left[ \frac{A}{\rho \bar{r} \omega^2} \right] P \quad (10)$$

The fluid capacitance in centrifugal system is  $C = \left[ \frac{A}{\rho \bar{r} \omega^2} \right]$ .

#### 4.4. Flow resistance

The flow resistance can be considered Ohm's law  $\Delta V = IR$ .

$$\Delta P = qR \quad (11)$$

Flow resistance of rectangular microchannel can be calculated using the following Fourier series [37].

$$R_h = \frac{12\eta L}{\left( 1 - \frac{h}{w} \left( \frac{192}{\pi^5} \sum_{n=1,2,3}^{\infty} \frac{1}{n^5} \tanh \left( \frac{n\pi w}{2h} \right) \right) \right)} \omega h^3 \quad (12)$$

$$P = I\dot{q}$$

Also, flow resistance by rectangular cross section for  $h/w \ll 1$  can be approximated [31]:

$$R_h = \frac{12\eta L}{\omega h^3} \quad (13)$$

where  $w$  is width and  $h$  height of the channel.

#### 4.5. Inertance

Newton's second law that is called the linear momentum relation of fluid flow in the channel is [38]:

$$\sum \vec{F} = \frac{d(m\vec{V})}{dt} \quad (14)$$

$$A(P_1 - P_2) = m\dot{v} = \rho LA\dot{v} \quad (15)$$

$$\Delta P = \frac{\rho L}{A} \dot{q} \quad (16)$$

This relation is similar to inductor equation  $\Delta V = L \frac{di}{dt}$  and we could write where  $I = \rho L/A$  and  $p$  represents pressure difference.

#### 4.6. Application example

In this work, we consider a single design which allows us to demonstrate how our lumped-element approach can be applied to "digital" centrifugal flow control. Therefore, we model a liquid handling protocol similar to that used by Nwankire et al. [35] to implement a nitrite/nitrate panel for whole blood monitoring. To implement their assay, Nwankire et al. used DF burst valves which were designed to open in sequence with increasing spin rate of the disc. We present a lumped-element model to simulate the centrifugo-pneumatic chambers which are the key enabling technology of the DF burst valves; a good understanding of these chambers is also critical to the implementation of our event-triggered valving architecture [22]. The schematic view of the design is shown in **Figure 4**. This design shows three reservoirs, labeled A through C and three pneumatic chambers which are sealed using DF burst valves. The DFs are arranged to burst at a rotational frequency greater than 20 Hz and less than 40 Hz. These reservoirs feed a mixing chamber which is further sealed by two DFs which dissolve

on contact with the liquid. Upon dissolution, an open path into two overflow reservoirs is provided.

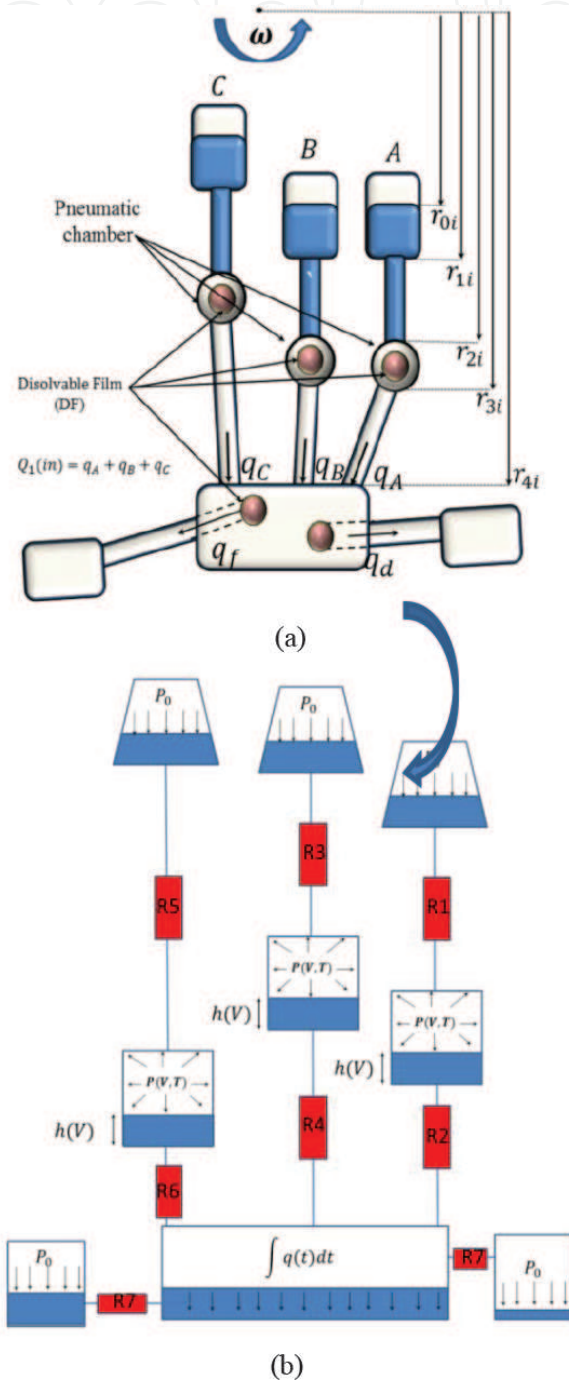


**Figure 4.** (a) The design of centrifugal microfluidic platform (b) Schematic view of Lumped element network.

We model the system in four different conditions to demonstrate a parallel simulation defined by different spin rates. These conditions share a spin profile (**Figure 5a**) which involves a rapid acceleration to a maximum frequency, followed by rapid mixing, stopping the disc, and then fast acceleration back to the maximum frequency. These spin protocols are identical except for their magnitude; they have maximum spin rates of 20 Hz, 40 Hz, 60 Hz, and 80 Hz.

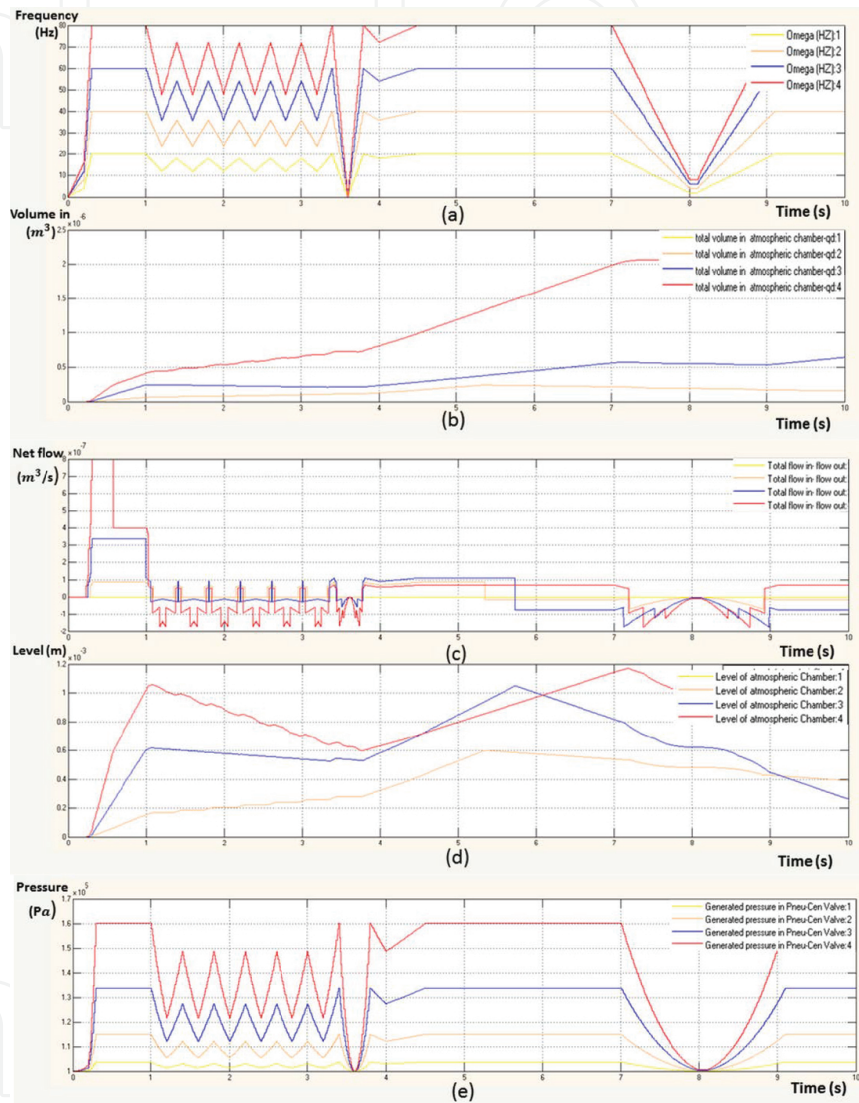


**Figure 5.** Lumped-element simulation graph for main atmospheric reservoir. (a) Angular frequency profile vs the time. (b) Total inflow vs time. (c) Total net flow (flow-in-flow-out) vs time. (d) Filling level of the chamber due to the ingress of liquid into the reservoir. (e) Pressure generated in the pneumatic and centrifugal valve (A) due to angular velocity.

To demonstrate the wide capability of this lumped-element model to predict on disc performance, a number of parameters are shown in **Figure 5** which have been calculated using the simulation software based on a number of defined boundaries and initial conditions. These parameters are the volume flow into the mixing chamber assuming no out volume flow through the two exits (**Figure 5b**); the net flow into the mixing chamber, assuming outflow

through the exists (**Figure 5c**); and the liquid level in the mixing chamber, assuming outflow through the exits (**Figure 5d**). Finally, Figure 5e shows the predicted pressure, during the spin profile, in each DF burst valve with the assumption the DF does not dissolve.

Based on the lumped-element analysis, the critical burst frequencies of the DFs are between 25 and 30 Hz. Therefore, in **Figure 5b, c, and d**, it is predicted that, for the 20 Hz test condition, the DFs do not dissolve and so there is no liquid flow. As stated above, Figure 5b shows the total volume entering into the main chamber; this is defined as  $V_{in} = V_A + V_B + V_C$ . Similarly, the net flow rate in and out of the mixing chamber is shown in **Figure 5c** and is defined by  $q_{net} = q_A + q_B + q_C - q_d - q_f$ . In turn, and most importantly, the liquid level in the main chamber can also be predicted in Figure 5d; this information is important as it can be used to inform incubation times and washing protocols which are critical for Lab-on-a-Disc applications.

Finally, in **Figure 5e**, the pressurization of the centrifugo-pneumatic valves (Valve A) is presented. Here, the increased centrifugal force pushes the liquids from the main reservoir (Reservoir A) and into the dead-end pneumatic chamber which is sealed by a DF. The fluid flow is stopped in the pneumatic chamber by a pocket of entrapped air which pushes back against the centrifugally generated hydrostatic pressure; this equilibrium condition is reached when the centrifugal pressure head, described previously in Eq. (4), balances with the pressure of the trapped gas, defined by Boyle's law in Eq. (6). In the real case, the DF membrane in the pneumatic chamber is dissolved (valve opening) beyond the critical burst frequency when the liquid ingress is sufficient to contact the film. Then, the liquid flows are directed into the main (downstream) chamber.

Over the past three decades, a special breed of microfluidic systems is based on centrifugal liquid handling for a wide spectrum of applications in biomedical point-of-care diagnostics and the life sciences. Recently, event-triggered flow control was introduced on these LoAD platforms to implement logical flow control which functions akin to digital microelectronics [33]. Similar to the difference between an old-fashioned office mainframe and a modern smartphone, these breakthroughs may provide an unprecedented level of system integration and automation which is needed to eventually implement complex, highly functional networks representing a repertoire of bioanalytical assays on a user-friendly, cost-efficient, portable, and still high-performance microfluidic point-of-use "gadget." We presented an advanced lumped-element approach for the fast-generation and robust simulation for event-triggered centrifugal microfluidic networks.

## Author details

Mahdi Mohammadi, David J Kinahan and Jens Ducreé\*

\*Address all correspondence to: jens.ducree@dcu.ie

School of Physical Sciences, National Centre for Sensor Research, Dublin City University (DCU), Dublin, Ireland

## References

- [1] J. Ducreé, S. Haerberle, S. Lutz, S. Pausch, F. Von Stetten, and R. Zengerle, "The centrifugal microfluidic Bio-Disk platform," *J. Micromechanics Microengineering*, vol. 17, no. 7, pp. S103–S115, 2007.
- [2] S. Smith, D. Mager, A. Perebikovskiy, E. Shamloo, D. Kinahan, R. Mishra, S. Torres Delgado, H. Kido, S. Saha, J. Ducreé, M. Madou, K. Land, and J. Korvink, "CD-Based Microfluidics for Primary Care in Extreme Point-of-Care Settings," *Micromachines*, vol. 7, no. 2, p. 22, 2016.
- [3] O. Strohmeier, M. Keller, F. Schwemmer, S. Zehnle, D. Mark, F. von Stetten, R. Zengerle, and N. Paust, "Centrifugal microfluidic platforms: advanced unit operations and applications," *Chem. Soc. Rev.*, vol. 44, pp. 6187–6229, 2015.
- [4] R. Gorkin, J. Park, J. Siegrist, M. Amasia, B. S. Lee, J.-M. Park, J. Kim, H. Kim, M. Madou, and Y.-K. Cho, "Centrifugal microfluidics for biomedical applications," *Lab Chip*, vol. 10, pp. 1758–1773, 2010.
- [5] M. Madou, J. Zoval, G. Jia, H. Kido, J. Kim, and N. Kim, "Lab on a Cd," *Annu. Rev. Biomed. Eng.*, vol. 8, no. 1, pp. 601–628, 2006.
- [6] D. J. Kinahan, S. M. Kearney, N. Dimov, M. T. Glynn, and J. Ducreé, "Event-triggered logical flow control for comprehensive process integration of multi-step assays on centrifugal microfluidic platforms," *Lab Chip*, vol. 14, no. 13, pp. 2249–2258, 2014.
- [7] D. J. Kinahan, S. M. Kearney, O. P. Faneuil, M. T. Glynn, N. Dimov, and J. Ducreé, "Paper imbibition for timing of multi-step liquid handling protocols on event-triggered centrifugal microfluidic lab-on-a-disc platforms," *RSC Adv.*, vol. 5, no. 3, pp. 1818–1826, 2015.
- [8] M. Kong and E. Salin, "Pneumatic flow switching on centrifugal microfluidic platforms in motion," *Anal. Chem.*, vol. 83, pp. 1148–1151, 2011.
- [9] L. Clime, D. Brassard, M. Geissler, and T. Veres, "Active pneumatic control of centrifugal microfluidic flows for lab-on-a-chip applications," *Lab Chip*, vol. 15, no. 11, pp. 2400–11, 2015.
- [10] J. L. Garcia-Cordero, D. Kurzbuch, F. Benito-Lopez, D. Diamond, L. P. Lee, and A. J. Ricco, "Optically addressable single-use microfluidic valves by laser printer lithography," *Lab Chip*, vol. 10, no. 20, p. 2680, 2010.
- [11] B. S. Lee, Y. U. Lee, H.-S. H. Kim, T.-H. Kim, J. Park, J.-G. Lee, J. Kim, H.-S. H. Kim, W. G. Lee, and Y.-K. Cho, "Fully integrated lab-on-a-disc for simultaneous analysis of biochemistry and immunoassay from whole blood," *Lab Chip*, vol. 11, no. 1, pp. 70–78, 2011.

- [12] K. Abi-Samra, R. Hanson, M. Madou, and R. a Gorkin, "Infrared controlled waxes for liquid handling and storage on a CD-microfluidic platform.," *Lab Chip*, vol. 11, no. 4, pp. 723–726, 2011.
- [13] W. Al-Faqheri, F. Ibrahim, T. H. G. Thio, J. Moebius, K. Joseph, H. Arof, and M. Madou, "Vacuum/Compression Valving (VCV) Using Paraffin-Wax on a Centrifugal Microfluidic CD Platform," *PLoS One*, vol. 8, no. 3, pp. 2–10, 2013.
- [14] T. Kawai, N. Naruishi, H. Nagai, Y. Tanaka, Y. Hagihara, and Y. Yoshida, "Rotatable reagent cartridge for high-performance microvalve system on a centrifugal microfluidic device," *Anal. Chem.*, vol. 85, no. 14, pp. 6587–6592, 2013.
- [15] M. Geissler, L. Clime, X. D. Hoa, K. J. Morton, H. Hébert, L. Poncelet, M. Mounier, M. Deschênes, M. E. Gauthier, G. Huszczyński, N. Corneau, B. W. Blais, and T. Veres, "Microfluidic Integration of a Cloth-Based Hybridization Array System (CHAS) for Rapid, Colorimetric Detection of Enterohemorrhagic Escherichia coli (EHEC) Using an Articulated, Centrifugal Platform," *Anal. Chem.*, vol. 87, no. 20, pp. 10565–10572, 2015.
- [16] B. Miao, N. Peng, L. Li, Z. Li, F. Hu, Z. Zhang, and C. Wang, "Centrifugal Microfluidic System for Nucleic Acid Amplification and Detection," *Sensors*, vol. 15, no. 11, pp. 27954–27968, 2015.
- [17] T. Li, L. Zhang, K. M. Leung, and J. Yang, "Out-of-plane microvalves for whole blood separation on lab-on-a-CD," *J. Micromechanics Microengineering*, vol. 20, no. 10, p. 105024, 2010.
- [18] S. Haerberle, T. Brenner, R. Zengerle, and J. Ducee, "Centrifugal extraction of plasma from whole blood on a rotating disk.," *Lab Chip*, vol. 6, no. 6, pp. 776–781, 2006.
- [19] T. H. G. Thio, S. Soroori, F. Ibrahim, W. Al-Faqheri, N. Soin, L. Kulinsky, and M. Madou, "Theoretical development and critical analysis of burst frequency equations for passive valves on centrifugal microfluidic platforms.," *Med. Biol. Eng. Comput.*, vol. 51, no. 5, pp. 525–35, 2013.
- [20] J. L. Moore, A. McCuiston, I. Mittendorf, R. Ottway, and R. D. Johnson, "Behavior of capillary valves in centrifugal microfluidic devices prepared by three-dimensional printing," *Microfluid. Nanofluidics*, vol. 10, no. 4, pp. 877–888, 2011.
- [21] J. M. Chen, P. C. Huang, and M. G. Lin, "Analysis and experiment of capillary valves for microfluidics on a rotating disk," *Microfluid. Nanofluidics*, vol. 4, no. 5, pp. 427–437, 2008.
- [22] R. Gorkin, C. E. Nwankire, J. Gaughran, X. Zhang, G. G. Donohoe, M. Rook, R. O'Kennedy, and J. Ducee, "Centrifugo-pneumatic valving utilizing dissolvable films," *Lab a Chip - Miniaturisation Chem. Biol.*, vol. 12, no. 16, pp. 2894–2902, 2012.
- [23] C. E. Nwankire, M. Czugala, R. Burger, K. J. Fraser, T. M. Connell, T. Glennon, B. E. Onwuliri, I. E. Nduaguibe, D. Diamond, and J. Ducee, "A portable centrifugal analyser for liver function screening," *Biosens. Bioelectron.*, vol. 56, pp. 352–358, 2014.



- [24] T. van Oordt, Y. Barb, J. Smetana, R. Zengerle, and F. von Stetten, "Miniature stick-packaging – an industrial technology for pre-storage and release of reagents in lab-on-a-chip systems," *Lab Chip*, vol. 13, no. 15, p. 2888, 2013.
- [25] H. Hwang, H.-H. Kim, and Y.-K. Cho, "Elastomeric membrane valves in a disc.," *Lab Chip*, vol. 11, no. 8, pp. 1434–1436, 2011.
- [26] D. Mark, P. Weber, S. Lutz, M. Focke, R. Zengerle, and F. Von Stetten, "Aliquoting on the centrifugal microfluidic platform based on centrifugo-pneumatic valves," *Microfluid. Nanofluidics*, vol. 10, no. 6, pp. 1279–1288, 2011.
- [27] C. E. Nwankire, G. G. Donohoe, X. Zhang, J. Siegrist, M. Somers, D. Kurzbuch, R. Monaghan, M. Kitsara, R. Burger, S. Hearty, J. Murrell, C. Martin, M. Rook, L. Barrett, S. Daniels, C. McDonagh, R. O'Kennedy, and J. Ducreé, "At-line bioprocess monitoring by immunoassay with rotationally controlled serial siphoning and integrated super-critical angle fluorescence optics.," *Anal. Chim. Acta*, vol. 781, no. 4, pp. 54–62, 2013.
- [28] J. Siegrist, R. Gorkin, L. Clime, E. Roy, R. Peytavi, H. Kido, M. Bergeron, T. Veres, and M. Madou, "Serial siphon valving for centrifugal microfluidic platforms," *Microfluid. Nanofluidics*, vol. 9, no. 1, pp. 55–63, 2010.
- [29] M. Kitsara, C. E. Nwankire, L. Walsh, G. Hughes, M. Somers, D. Kurzbuch, X Zhang, G. G. Donohoe, R. O'Kennedy, and J. Ducreé, "Spin coating of hydrophilic polymeric films for enhanced centrifugal flow control by serial siphoning," *Microfluid. Nanofluidics*, vol. 16, no. 4, pp. 691–699, 2014.
- [30] M. M. Aeinehvand, F. Ibrahim, S. W. harun, W. Al-Faqheri, T. H. G. Thio, A. Kazemzadeh, and M. Madou, "Latex micro-balloon pumping in centrifugal microfluidic platforms," *Lab Chip*, vol. 14, no. 5, p. 988, 2014.
- [31] F. Schwemmer, S. Zehnle, D. Mark, F. von Stetten, R. Zengerle, and N. Paust, "A microfluidic timer for timed valving and pumping in centrifugal microfluidics," *Lab Chip*, vol. 15, no. 6, pp. 1545–1553, 2015.
- [32] N. Godino, R. Gorkin, A. V Linares, R. Burger, and J. Ducreé, "Comprehensive integration of homogeneous bioassays via centrifugo-pneumatic cascading.," *Lab Chip*, vol. 13, no. 4, pp. 685–94, 2013.
- [33] R. Gorkin, L. Clime, M. Madou, and H. Kido, "Pneumatic pumping in centrifugal microfluidic platforms," *Microfluid. Nanofluidics*, vol. 9, no. 2–3, pp. 541–549, 2010.
- [34] C. E. Nwankire, A. Venkatanarayanan, T. Glennon, T. E. Keyes, R. J. Forster, and J. Ducreé, "Label-free impedance detection of cancer cells from whole blood on an integrated centrifugal microfluidic platform.," *Biosens. Bioelectron.*, vol. 68C, no. November, pp. 382–389, 2014.
- [35] C. Nwankire, D.-S. Chan, J. Gaughran, R. Burger, R. Gorkin, and J. Ducreé, "Fluidic Automation of Nitrate and Nitrite Bioassays in Whole Blood by Dissolvable-Film Based Centrifugo-Pneumatic Actuation," *Sensors*, vol. 13, no. 9, pp. 11336–11349, 2013.

- [36] R. Z. and P. K. C. Litterst, W. Streule, "Simulation Toolkit for Micro Fluidic Pumps Using Lumped Element Model," vol. 1, pp. 736–739, 2005.
- [37] K. W. Oh, K. Lee, B. Ahn, and E. P. Furlani, "Design of pressure-driven microfluidic networks using electric circuit analogy," *Lab Chip*, vol. 12, no. 3, pp. 515–545, 2012.
- [38] F. White, *Fluid Mechanics*, McGraw-Hill, New York, NY, USA: 3–225. 1999.

IntechOpen

IntechOpen

